Seismic Response of Precast Prestressed Concrete Frames With Partially Debonded Tendons

M. J. Nigel Priestley, Ph.D.
Professor of Structural Engineering
University of California, San Diego
La Jolla, California

The concept of connecting precast concrete frame elements with beam prestressing tendons debonded through the joint, and for some distance on either side of the column, is discussed. It is shown that improved joint shear performance and restoring force characteristics can be expected from this arrangement. Results of dynamic inelastic analyses indicate that for structures with long natural periods, peak displacement response should be similar to that of conventionally prestressed concrete systems, and only slightly larger than systems with elasto-plastic hysteretic characteristics. A numerical design example is provided in an Appendix to show how the force-deformation characteristics of precast concrete frame systems utilizing this concept may be calculated.

Jian Ren Tao, Ph.D.
Research Engineer
SC Solutions, Inc.
Mt. View, California

Precast concrete frames, using beam elements connected to multistory column elements with post-tensioned prestressing tendons, have been identified as an economically viable method of construction for tall buildings.[1] Recent research at the National Institute of Standards and Technology (NIST)[2] has indicated that beam-to-column joint subassemblages using fully grouted tendons developed ductility comparable to monolithic reinforced concrete subassemblages designed according to current Uniform Building Code (UBC) specifications.[3] However, after moderate ductility levels had been achieved, these subassemblages suffered excessive stiffness degradation

at low displacements. This degradation was caused by a reduction of effective prestress clamping force through the column, resulting from inelastic strain of the prestressing tendon at the critical section. This behavior is shown in idealized form in Fig. 1, which refers to a typical prestressing steel stress-strain curve.

In Fig. 1, f_{si} is the initial steel stress after prestress losses. During low-level seismic response, fluctuations of the steel stress will be within the elastic range, and no loss of prestress will result when deformations return to zero. At a ductility level of (say) $\mu = 2$, represented by Point 2 in Fig. 1, the maximum prestressing steel response is expected to be on the inelastic por-
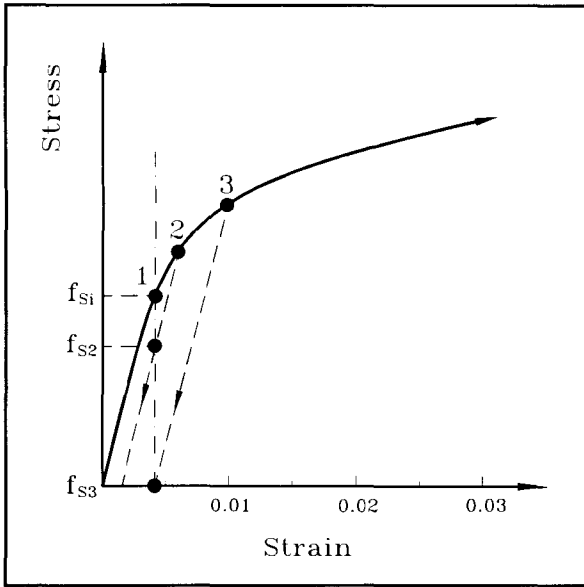
Fig. 1. Prestress loss due to inelastic response.

Fig. 2. Hysteretic response of a precast, prestressed beam-to-column joint subassemblage.[2] (Note: 1 kip = 4.45 kN; 1 in. = 25.4 mm.)

tion of the stress-strain curve.

On unloading, the steel follows a linear descending branch essentially parallel to the initial modulus of elasticity. Hence, when the structure returns to zero deformation, the effective steel stress is reduced to f_{s2}. On unloading from higher ductility levels, involving larger inelastic strains as indicated by Point 3 on Fig. 1, the entire prestress may be lost. This is clearly undesirable when the surfaces between the precast concrete beam and column are planar, and rely on prestress shear friction to transmit the gravity shear forces from beam to column.

The result is excessive pinching of the force-deflection hysteresis loops, as indicated by the typical prestress loops from the NIST tests shown in Fig. 2. It should be noted that gravity loads on the beams were not modeled in these tests. Similar results were obtained in earlier tests of monolithic prestressed concrete construction by Blakeley and Park[4] and Thompson and Park.[5] They found that improved hysteretic performance could be obtained from units with additional mild steel flexural reinforcement. Also, they found that the behavior would be improved if the prestress force was concentrated in the central region of the beam depth, in order to minimize inelastic prestress strains.

The second option can be adopted for precast assemblages, and involves no significant penalty in terms of flex-

ural strength compared with the same prestress force distributed through the beam depth or concentrated in tendons near the top and bottom beam surfaces. This is because the moment capacity is provided by an increased tension force acting at a reduced lever arm, compared with a beam where half of the prestress force is close to the compression zone, and relatively ineffective for moment considerations. However, placing mild steel reinforcement across the connection between precast concrete elements would result in cost and time increases, thus making precast concrete construction less competitive compared with alternative forms of construction.

PARTIALLY DEBONDED TENDONS

The use of unbonded prestressing tendons in frame construction has been considered by Ishizuka[6] (under the supervision of Hawkins) who tested partially prestressed monolithic frame joints. However, unbonded tendons are not recommended for seismic regions because of poor anchorage performance in earlier earthquakes. The use of partially debonded tendons where the tendon is debonded through the joint and for some distance on either side, as indicated in Fig. 3, would appear to have the following advantages:

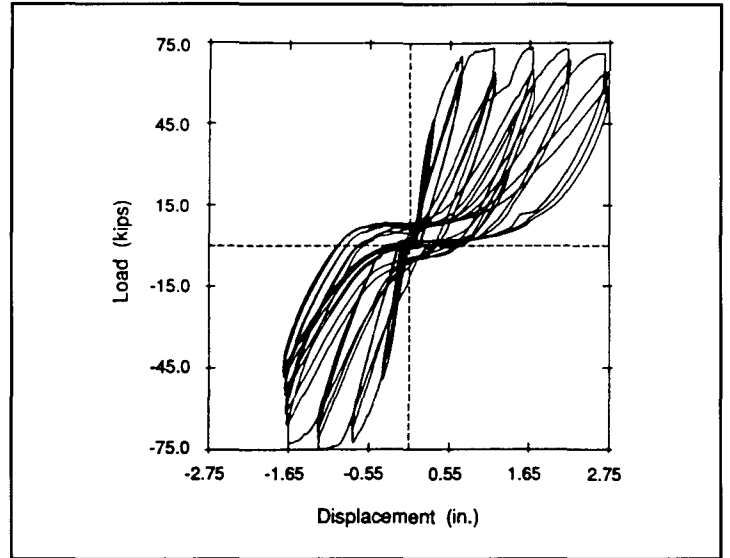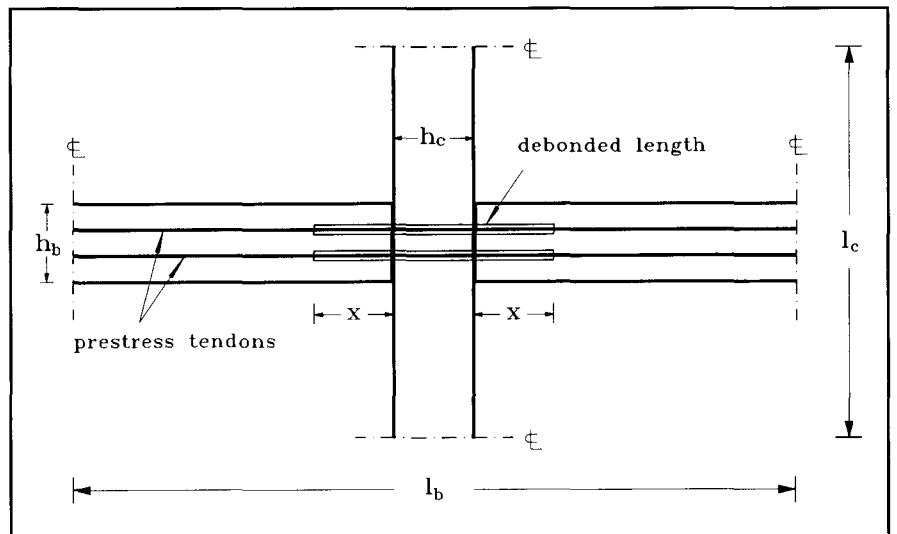**1.** If the length of debonding is cor-

Fig. 3. Interior precast concrete beam-to-column unit with partially debonded tendons.

rectly chosen, the required ultimate displacement could be achieved without exceeding the limit of proportionality of the prestressing steel. Consequently, there would be no loss of prestress on unloading from the design level of ductility. Shear friction on the beam-to-column interfaces would be maintained at all response levels, and support of gravity load shear would not be jeopardized.

2. The response would be essentially elastic, though nonlinear, as discussed subsequently. Although this would have possibly undesirable consequences for energy absorption, it has the merit that, following response to the design level earthquake, the structure would return to its original position without residual displacement, and the initial stiffness would be restored.

3. Design of the beam-to-column joint region should be greatly simplified, since the entire horizontal joint shear forces would be fully transferred by a diagonal compression strut, as shown in Fig. 4. This is a consequence of the prestress tensile forces on either side of the joint being equal for each tendon, because the tendons are debonded through the joint.

Thus, no special horizontal reinforcement would be needed to transfer joint forces. Assuming the column

was designed to remain elastic under seismic actions, with reinforcement distributed on the sides, it is also probable that no special vertical joint shear reinforcement would be needed. Joint reinforcement could, thus, consist of essentially nominal transverse hoops.

There are, of course, potentially undesirable characteristics resulting from the debonded design. As noted previously, there will be little energy dissipation since the prestress is expected to remain in the elastic range of material response. Wide cracks are to be expected at the beam-to-column interfaces, and the associated compression strains above (or below) the cracks are likely to be large. Therefore, some special beam confinement reinforcement may be necessary.

LATERAL FORCE-DEFLECTION CHARACTERISTICS

Force-deflection characteristics of a typical debonded precast, prestressed concrete joint are indicated in Fig. 5(b), based on the forces and displacements measured at the tip of a beam-to-column subassemblage, as shown in Fig. 5(a).

Assuming no tension capacity across the beam-to-column interface, nonlinearity of response will initiate

at Point 1 when the precompression at the extreme compression fiber is lost and a crack starts to propagate. Assuming further that the prestress centroid is at the beam midheight, the corresponding moment is:

$$M_{cr} = \frac{T_i h_b}{6} \qquad (1)$$

for a rectangular section, where T_i is the initial total prestressing force.

For the dimensions shown in Figs. 3 and 5, the corresponding lateral force F will be:

$$F_{cr} = \frac{2\,M_{cr}\ell_b}{(\ell_b - h_c)\ell_c} \qquad (2)$$

The corresponding displacement can be found from a simple linear elastic analysis based on uncracked section properties. Deviation from the initial linear elastic force-deformation characteristic will be minimal until the crack has propagated at least to the centroidal axis of the beam, unless the average prestress level is fairly high $(f_{pc} > 0.25f'_c)$. This is because prestressing steel strains will change very little.

When the crack has propagated to the centroidal axis, corresponding to Point 2 in Fig. 5(b), the moment will be:

$$M_2 \approx \frac{T_i h_b}{3} = 2M_{cr} \qquad (3)$$

Above this point, the precise force-deflection relationship is difficult to determine, since steel strains and concrete strains are not linearly related. However, it is relatively simple to determine the force and displacement at Point 3, corresponding to the limit of proportionality on the steel stress-strain curve, since it is reasonable to assume at this stage that concrete ultimate conditions are approached. This allows an equivalent ultimate compression stress block to be utilized.

It should be noted that the compression stress block parameters are rather insensitive to the strain level as ultimate strain is approached; thus, any errors resulting from this assumption are likely to be minor. For example, with reference to Fig. 6, the moment of the equivalent compression stress block about the neutral axis is:
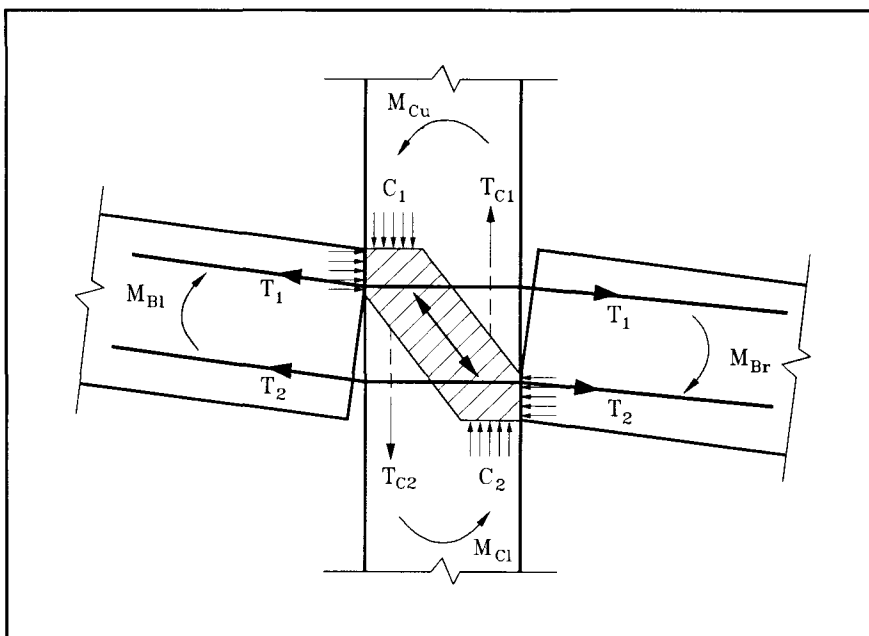

Fig. 4. Forces contributing to joint shears with partially debonded prestressing tendons.

$$M_c = \alpha\beta\left(1 - \frac{\beta}{2}\right)bc^2 f_c' \qquad (4)$$

As the shape of the compression stress block changes from the linear distribution corresponding to initial elastic conditions to ultimate conditions, which may be represented by the ACI rectangular block for normal strength concrete, the product $\alpha\beta$ $(1 - \beta/2)$ changes only from 0.33 to 0.415. It follows that, providing the appropriate parameters for ultimate conditions for unconfined or confined conditions are met, this asumption will lead to negligible errors even if extreme fiber compression strains are not close to ultimate.

At the limit of proportionality of the prestressing steel stress-strain curve, the increase in steel strain will be:

$$\Delta\varepsilon_s = \frac{1}{E_s}\left(f_{slp} - f_{si}\right) \qquad (5)$$

where f_{slp} and f_{si} are the steel stresses at the limit of proportionality, and initially after strain losses, respectively.

Equating compression and tension forces, the neutral axis depth is given by:

$$c = \frac{A_{ps} f_{slp}}{\alpha\beta b f_{cc}'} \qquad (6)$$

where A_{ps} is the total area of prestressing steel, with a corresponding peak moment capacity of:

$$M_3 = A_{ps} f_{slp}\left(\frac{h_b}{2} - \frac{\beta c}{2}\right) \qquad (7)$$

and f_{cc}' is the compressive strength of the concrete, which is assumed to be confined, as discussed subsequently.

The corresponding lateral force is given by Eq. (2), substituting M_3 for M_{cr}.

The extension of the prestressing tendon from the column centerline to the end of the debonded region will be:

$$\Delta_\ell = \Delta\varepsilon_s\left(\frac{h_c}{2} + x\right) \qquad (8)$$

where x is the length of tendon debonding on either side of the column.

The corresponding rotation θ is thus approximately:

$$\theta = \frac{\Delta_\ell}{\dfrac{h_b}{2} - c} \qquad (9)$$

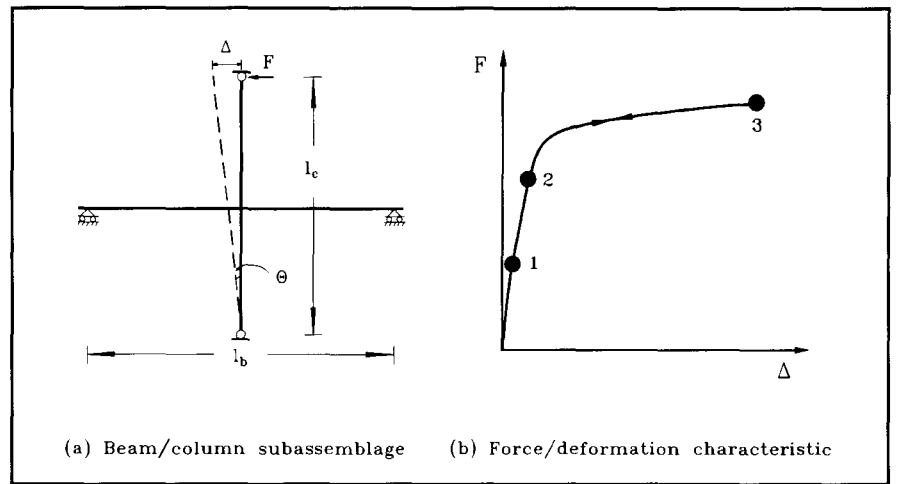(a) Beam/column subassemblage   (b) Force/deformation characteristic

Fig. 5. Force-deformation for an elastic partially debonded prestressed beam-to-column subassemblage.

Combining Eqs. (5), (8) and (9), and multiplying by ℓ_c, the lateral displacement at the top of the unit is:

$$\Delta_3 = A_2 \frac{M_3}{M_2} +$$

$$\frac{\ell_c}{E_s}\left(f_{slp} - f_{si}\right)\frac{(0.5h_c + x)}{(0.5h_b - c)} \qquad (10)$$

The force-deformation relationship described above may be conservatively approximated by an equivalent bilinear elastic relationship, as shown in Fig. 7, in which the force and displacement corresponding to Point 2 on Fig. 5(b) are taken as the equivalent yield conditions.

An equivalent displacement ductility capacity can be determined from:

$$\mu_\Delta = \frac{\Delta_u}{\Delta_y} = \frac{\Delta_3}{\Delta_2} \qquad (11)$$

Note that the "ultimate" displacement Δ_3 and the corresponding ductility will increase as the debonded length x increases, and the difference between initial stress, f_{si}, and, stress at limit of proportionality, f_{slp}, increases. Thus, it would appear advantageous to provide a comparatively low initial steel stress, perhaps just sufficient for gravity load considerations. It is again emphasized that the behavior in Fig. 7 is essentially elastic; that is, the unloading and loading curves are the same since inelastic steel strains do not occur.

It should also be noted that Eq. (11) does not define ductility in the conventional sense, since energy dissipation does not occur. Eq. (11) is the ratio between displacements at two limit states, representing the end of the two linear force-displacement states. The
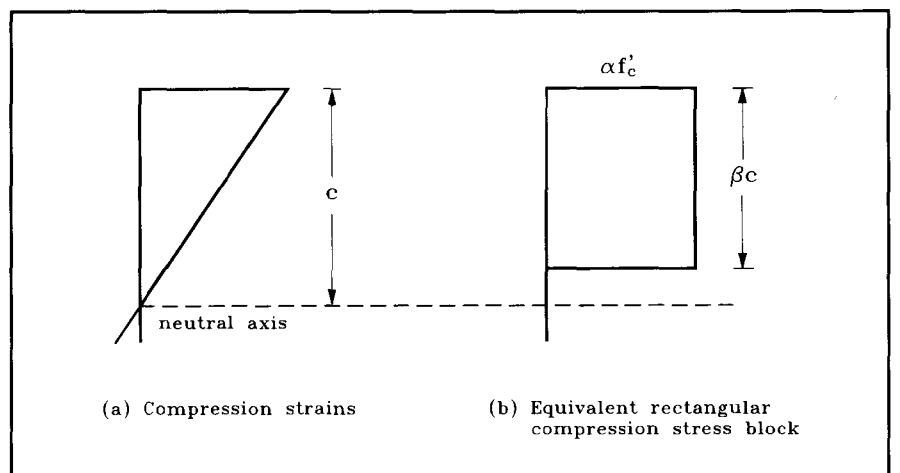

(a) Compression strains   (b) Equivalent rectangular compression stress block

Fig. 6. Definition of equivalent compression stress block.
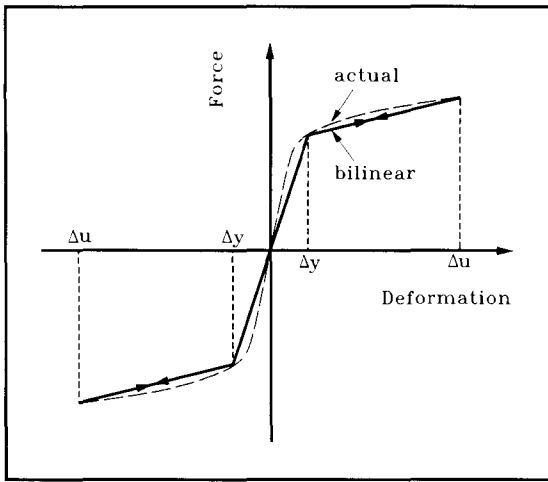
Fig. 7. Equivalent bilinear relationship.

Fig. 8. Beam end details.

BEAM HINGE CONFINEMENT

The relationship between steel strains and peak concrete compression strains is difficult to determine. However, it appears likely that high compression strains will develop in the beam ends in the plastic hinge region. As a consequence, conservative detailing of transverse reinforcement for confinement should be provided. Since only nominal longitudinal mild steel reinforcement will be placed in the beams, conventional rectangular hoops would provide only partial confinement.

It is, therefore, recommended that compression zones of rectangular precast concrete beams be confined by interlocking spirals, as shown in Fig. 8. The spirals should have the minimum cover permitted by code require-
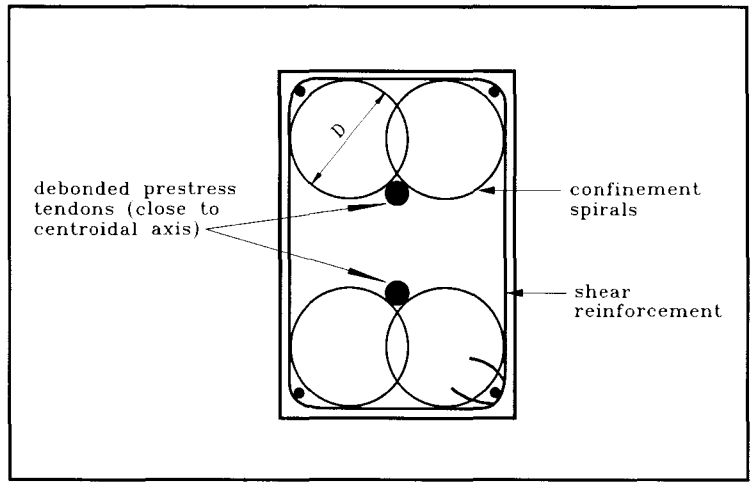
use of the term "ductility" is adopted for convenience, to enable direct comparison later between bilinear elastic and energy dissipating systems.

ments. Pending further experimental results, a volumetric ratio of confining steel of 2 percent, related to the spiral core area is suggested, with a spiral pitch not exceeding $D/4$, where D is the spiral diameter, to ensure a high effective ultimate compression strain.

Using the approach suggested by Mander et al.,[7] the compression strength of the confined concrete is given by:

$$f'_{cc} = f'_c \left[-1.254 \right.$$

$$\left. + 2.254 \sqrt{1 + \frac{7.94 f_\ell}{f'_c}} - \frac{2 f_\ell}{f'_c} \right] \quad (12)$$

where f_ℓ, the lateral confining stress, is related to the area A_{sp}, spiral diameter D and pitch s of the spiral confining steel by the relationship:

$$f_\ell = \frac{2 A_{sp} f_y}{D s} \quad (13)$$

The additional rectangular hoop reinforcement shown in Fig. 8 is required to provide necessary shear

strength. In this context, it should be noted that, since inelastic prestress strains are not expected, the normal contributions of the concrete shear resisting mechanism and of the prestress force should be dependable, even in the beam end regions.

Analysis of a precast, prestressed unit with debonded tendons is demonstrated by an example provided in Appendix B.

DYNAMIC RESPONSE OF SYSTEMS WITH DEBONDED TENDONS

Perhaps the biggest uncertainty associated with the concept developed here is the possible increase in lateral displacements as a consequence of the lack of hysteretic energy dissipation of the bilinear elastic force-deformation characteristic describing lateral response of debonded designs. To investigate this behavior, several single-degree-of-freedom oscillators of different initial natural periods and hysteretic characteristics were sub-

(a) Linear elastic   (b) Bilinear elastic   (c) Bilinear elastoplastic   (d) Bilinear degrading
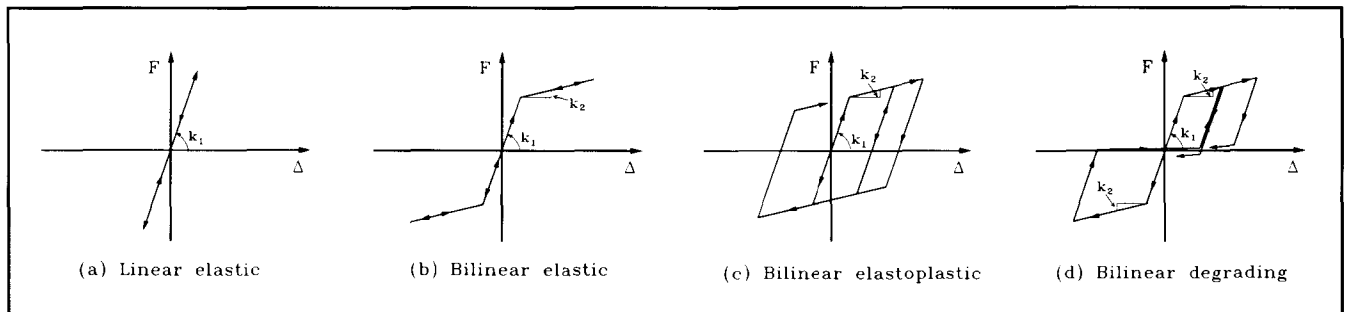
Fig. 9. Force-deflection characteristics for dynamic analyses.

jected to a range of different earthquake accelerograms using a time-history analysis procedure.

The accelerograms included El Centro 1940 NS, Taft 1952 S-69E, Orion Boulevard 1971 N-S, James Road 1979 N-1405, Loma Prieta 1989 N-S and Hachinohe 1968 N-S. In all cases, the accelerograms were scaled to give a peak ground acceleration of $0.4g$.

Force-deflection characteristics considered are shown schematically in Fig. 9. Fig. 9(a) represents linear elastic response of unlimited strength. Fig. 9(b) represents the idealized bilinear elastic response of the proposed debonded structural system. Fig. 9(c) represents an idealized bilinear elasto-plastic system. Lastly, Fig. 9(d) is an approximation of the response of bonded prestressed systems with severe stiffness degradation, as represented by the hysteretic loops of Fig. 2.

Initial elastic stiffnesses of the different models were adjusted to give periods of $T = 0.4, 0.8, 1.2, 1.6$ and 2.0 seconds. Strengths were based on UBC requirements for special reinforced concrete moment-resisting frames in Zone 4 on Type S2 soils, assuming a structural weight of 1000 kips (4450 kN).

Thus, the required yield strength was taken as:

$$F_y = 1.4W \left[\frac{0.4 \times 1.25S}{R_w T^{2/3}} \right]$$

where the force reduction factor $R_w = 12$, $S = 1.2$, T is the period and W is the weight.

Hence:

$$F_y = \frac{0.07}{T^{2/3}} W \qquad (14)$$

In all cases, 5 percent linear viscous damping and a second slope stiffness of $k_2 = 0.25k_1$ were assumed. Although this is reasonable for the bilinear elastic system, it is probably too high for the other nonlinear systems, which may result in the bilinear elastic case being unduly penalized.

RESULTS OF ANALYSES

Results from the analyses were prepared graphically in the form of displacement and shear force time-
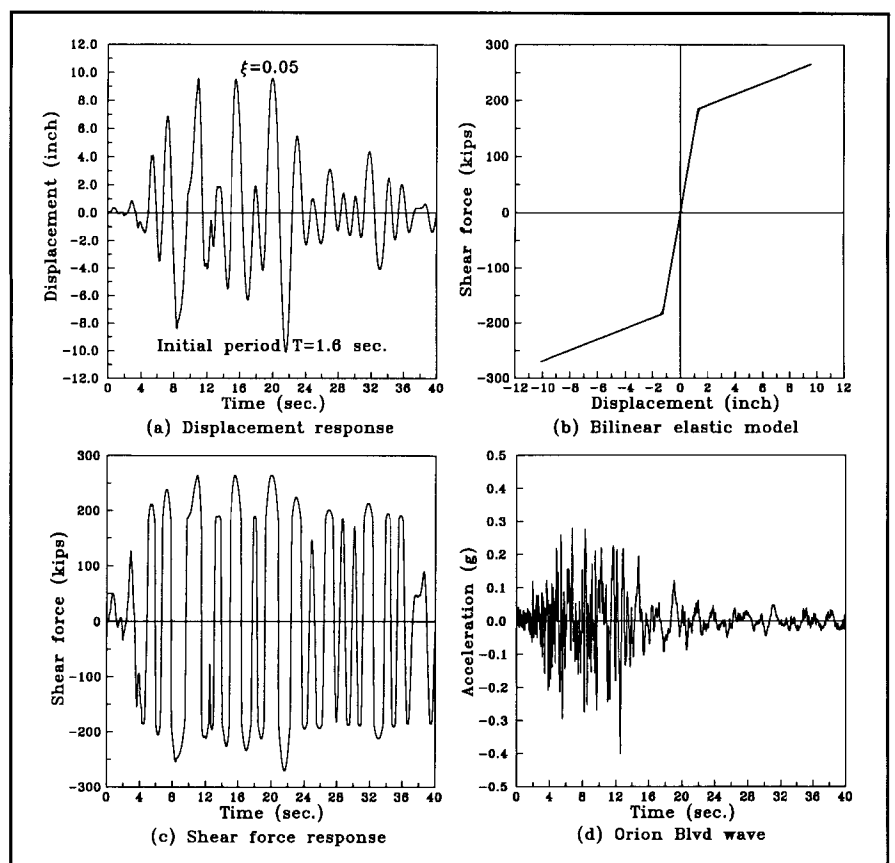

Fig. 10. Bilinear elastic response to Orion Boulevard record, $T = 1.6$ seconds. (Note: 1 kip = 4.45 kN; 1 in. = 25.4 mm.)
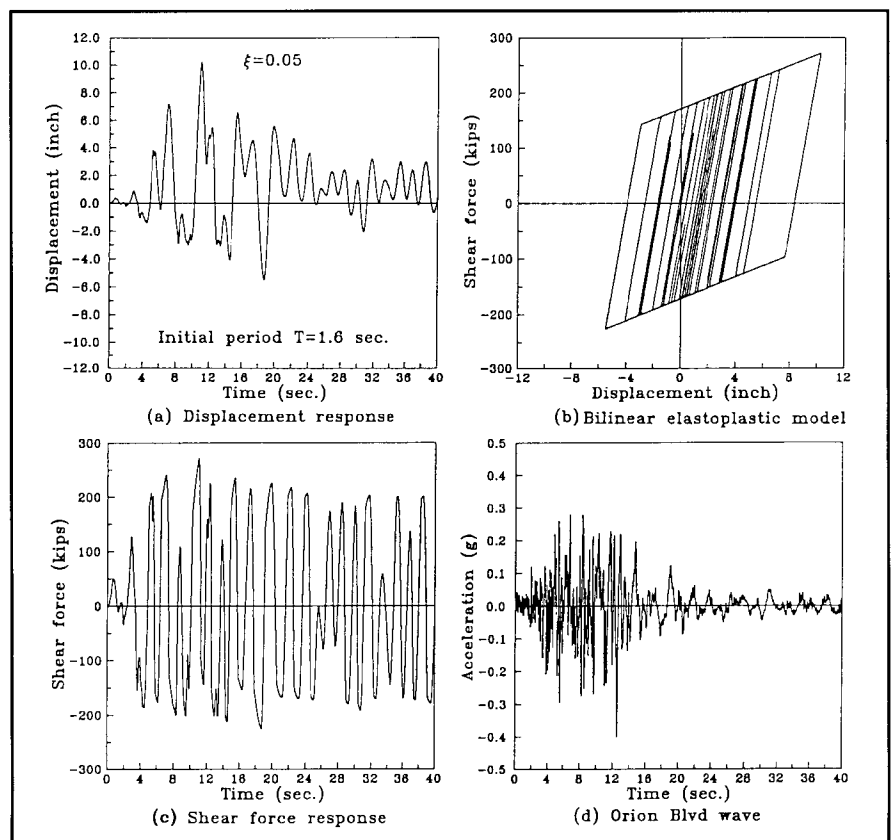

Fig. 11. Bilinear elasto-plastic response to Orion Boulevard record, $T = 1.6$ seconds. (Note: 1 kip = 4.45 kN; 1 in. = 25.4 mm.)
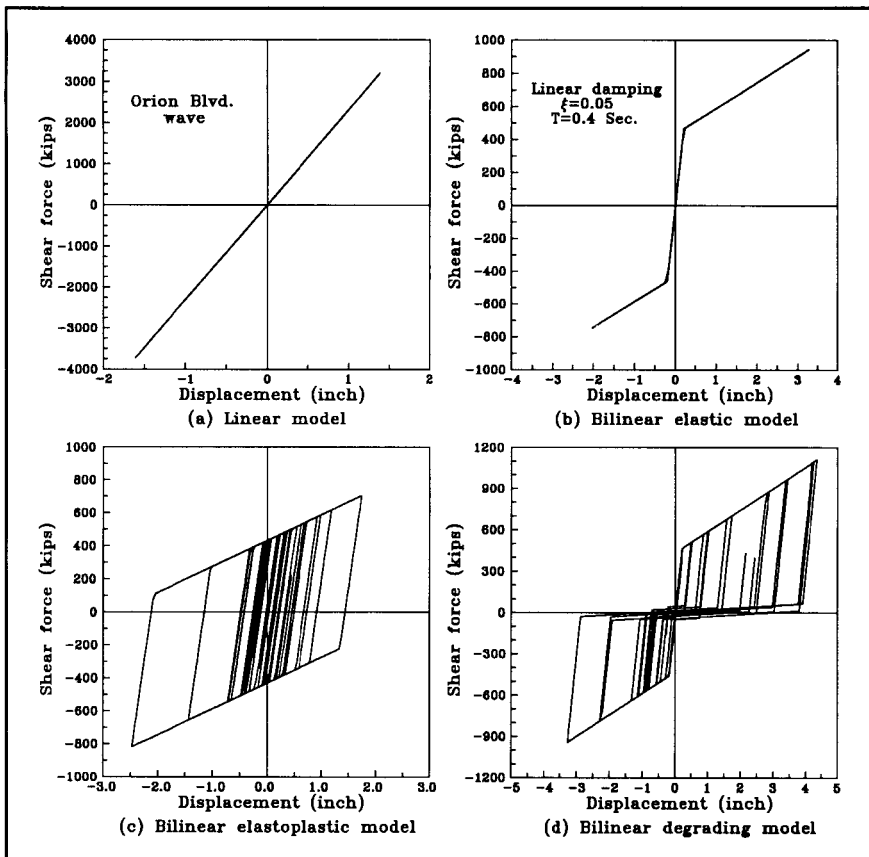
Fig. 12. Comparative response to Orion Boulevard record, T = 0.4 seconds. (Note: 1 kip = 4.45 kN; 1 in. = 25.4 mm.)
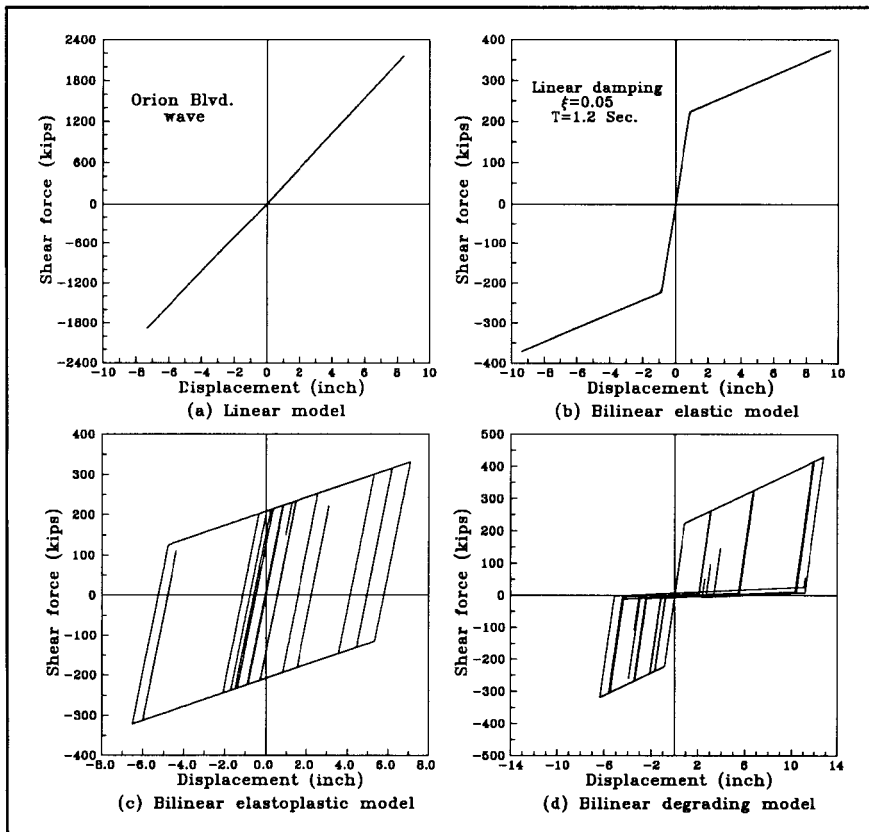

Fig. 13. Comparative response to Orion Boulevard record, T = 1.2 seconds. (Note: 1 kip = 4.45 kN; 1 in. = 25.4 mm.)

histories, and trajectories of shear force vs. displacement. Examples for the severe Orion Boulevard trace for bilinear elastic and elasto-plastic cases with T = 1.6 seconds are shown in Figs. 10 and 11, respectively.

For comparative purposes, the shear force-displacement plots for response of the four deformation characteristics for a given period and accelerogram were plotted on one graph. This is shown in Figs. 12 to 14 for the Orion Boulevard accelerogram, for T = 0.4, 1.2 and 2.0 seconds, respectively.

It can be seen that no consistent trend is discernable, except that elastic linear and bilinear elasto-plastic systems tend to have slightly lower peak response levels than the bilinear elastic and degraded hysteretic model. Of particular importance is the fact that displacement response for the bilinear elastic model is generally less than that for the degraded hysteretic model approximating the behavior of bonded prestressed beam-to-column assemblages.

A summary of responses in terms of ductility demand for all cases analyzed is provided in Table 1. All peak displacements, including the linear elastic case, have been divided by the nominal yield displacement corresponding to the common "corner" value of the three nonlinear cases shown in Fig. 9. These ductility demands can be compared with the value of $R_w/1.4$ = 8.6 implied by the "equal displacement" approximation of structural dynamic response and the value of $3R_w/8$ = 4.5 implied by UBC drift computation equations. Table 1 also includes the average of all earthquake records for a given hysteretic model and period.

The results show trends which have been observed before, namely, that structures designed to UBC exhibit decreasing displacement ductility demand with increasing period, and that the equal displacement approximation for elasto-plastic systems is nonconservative for short period structures and conservative for longer period structures. However, only for T = 2.0 seconds is the ductility demand less, on average, than the $3R_w/8$ implied by UBC. Of more interest here is the comparison of the two "prestressed" loops, with each

other and with the idealized elasto-plastic response.

An examination of Table 1 shows that there is no consistent difference in response levels sustained by the bilinear elastic and bilinear degraded hysteretic models. For short periods, the ductility demand is excessive for both models, exceeding 15, on average, at $T = 0.4$ seconds. However, for $T = 1.2$ seconds or greater, the ductility demand is not excessive, decreasing for the bilinear elastic case from 8.1 (on average) at $T = 1.2$ seconds to 5.8 at $T = 2.0$ seconds. Ductility demand exceeds that for the idealized elastoplastic model by 38 percent (on average) for $T \geq 1.2$ seconds. This result is similar to that reported by Thompson and Park[5] for conventionally prestressed structures. The ductility demands in Table 1 may be compared with the ductility capacity of 15.6 computed for the example considered in Appendix B. It would thus appear feasible to design structures using the debonded tendon concept.

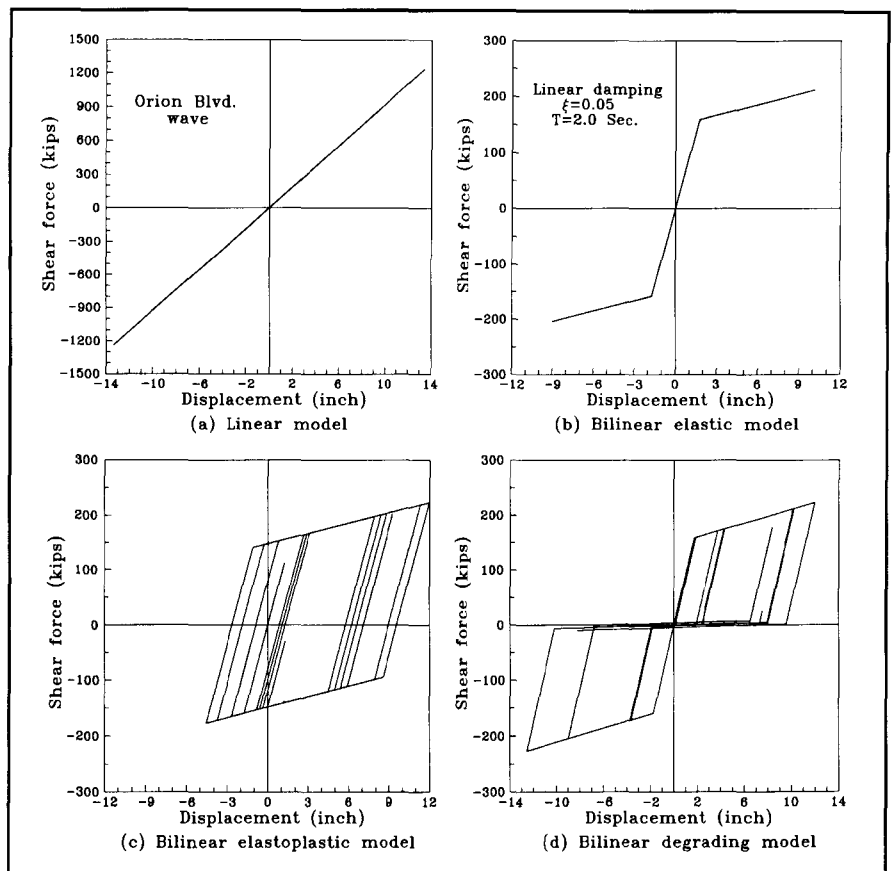It should be noted that the 38 percent ductility margin between bilinear elas-

Fig. 14. Comparative response to Orion Boulevard record, $T = 2.0$ seconds.
(Note: 1 kip = 4.45 kN; 1 in. = 25.4 mm.)

Table 1. Displacement ductility demands for different force-deformation characteristics.

Earthquake Record Model	El Centro* 1940 NS	Taft* 1952	Corroletis* 1989	James Rd* 1979	Orion Blvd.* 1971	Hachinohe* 1968	Avg.
$T = 0.4$							
Linear[†]	5.5	6.1	5.4	7.7	8.1	8.0	6.8
Bilinear elastic	19.2	12.7	19.1	11.4	16.4	26.2	17.5
Bilinear plastic	7.8	7.1	7.8	5.3	12.4	10.0	8.4
Bilinear degraded	16.7	14.3	13.1	9.4	20.0	20.6	15.7
$T = 0.8$							
Linear	7.9	7.8	13.7	4.6	8.6	8.5	8.5
Bilinear elastic	7.5	4.3	10.4	8.3	19.3	16.7	11.1
Bilinear plastic	5.8	5.6	6.3	5.2	10.1	8.2	6.9
Bilinear degraded	10.2	5.6	7.1	8.1	20.0	15.8	11.1
$T = 1.2$							
Linear	6.1	2.6	5.7	4.4	9.6	6.6	5.8
Bilinear elastic	4.9	4.6	4.7	7.9	10.9	15.4	8.1
Bilinear plastic	5.5	2.7	5.8	4.3	8.1	6.9	5.6
Bilinear degraded	6.0	4.8	4.0	7.7	15.8	15.5	9.0
$T = 1.6$							
Linear	4.4	2.8	4.4	3.9	10.5	4.2	5.0
Bilinear elastic	6.5	2.8	3.6	8.0	7.5	11.6	6.7
Bilinear plastic	4.1	2.8	2.6	5.9	8.1	5.6	4.9
Bilinear degraded	4.6	4.5	2.4	6.9	11.1	10.6	6.7
$T = 2.0$							
Linear	4.6	3.1	2.3	4.0	7.8	7.3	4.9
Bilinear elastic	6.8	6.2	2.1	6.5	5.9	7.5	5.8
Bilinear plastic	3.4	3.5	1.7	5.2	7.0	4.9	4.3
Bilinear degraded	5.0	4.6	2.4	5.9	7.4	7.9	5.5

* Scaled to 0.4g peak ground acceleration. [†] Related to yield displacement of other loops.

tic and bilinear elasto-plastic may not be appropriate for a comparison between reinforced concrete and the bilinear elastic prestressed model. Reinforced concrete members will have a less ideal hysteretic response than the elasto-plastic response, and the bilinear elastic response is likely to have higher damping than the 5 percent equivalent viscous model assumed for this study. Consequently, the difference in displacement between a monolithic reinforced concrete frame and a precast, prestressed concrete frame with debonded tendons is expected to be significantly less than 38 percent.

CONCLUSIONS

The concept of connecting precast concrete beam and column elements by using beam prestressing tendons debonded through the joint and for a distance on either side should result in the maintenance of prestress compressions even after large seismic displacements have occurred. Residual displacements should be negligible after a design level earthquake, and the residual stiffness at low displacements should remain close to the initial value. The concept should reduce joint shear stresses, resulting in a requirement for only nominal stirrups. A further consequence of the concept should be that dependable concrete shear resisting mechanisms exist in the beam plastic hinge regions at all ductility levels.

To ensure satisfactory performance of the beam plastic hinge regions, it is recommended that special spiral reinforcement, with a minimum volumetric ratio of 2 percent, be placed in the beam end regions for a distance equal to the beam depth from the column faces.

Extensive dynamic inelastic analyses show that ductility demands for structures with partially debonded tendons would be no greater than for fully bonded tendons where prestress degrades as a consequence of inelastic strains of the prestressing tendon. Although for short period structures high displacement ductility demands can be expected, the response of medium to long period prestressed concrete frames with debonded tendons should not exceed that for equivalent monolithic reinforced concrete frames by significant margins. Since the concept is most appropriate for structures higher than six stories, the high ductility demand for low period structures should not be a problem.

Experimental research is needed to confirm the actual shape of the force-deformation characteristic and available ductility capacity. A program of tests based on the concept is planned at the National Institute of Standards and Technology.

ACKNOWLEDGMENT

REFERENCES

1. Stanton, J. F., and Nakaki, S. D., "PRESSS Industry Seismic Workshops," PRESSS Report No. 91/2, October 1991.
2. Cheok, G. S., and Lew, H. S., "Performance of Precast Concrete Beam-to-Column Connections Subject to Cyclic Loading," PCI JOURNAL, V. 36, No. 3, May-June 1991, pp. 56-67.
3. ICBO, Uniform Building Code, 1991 Edition, International Conference of Building Officials, Whittier, CA.
4. Blakeley, R. W. G., and Park, R., "Prestressed Concrete Sections with Cyclic Flexure," Journal of the Structural Division, ASCE, V. 99, No. ST8, August 1973, pp. 1717-1742.
5. Thompson, K. J., and Park, R., "Ductility of Concrete Frames Under Seismic Loading," Department of Civil Engineering Report 75-14, University of Canterbury, New Zealand, October 1975.
6. Ishizuka, T., "Effect of Bond Deterioration on Seismic Response of Reinforced and Partially Prestressed Concrete Ductile Moment-Resisting Frames," Ph.D. Thesis, University of Washington, Seattle, WA, 1987.
7. Mander, J. B., Priestley, M. J. N., and Park, R., "Theoretical Stress-Strain Relationship for Confined Concrete," Journal of the Structural Division, ASCE, V. 114, No. 8, August 1988, pp. 1827-1849.

APPENDIX A — NOTATION

A_{ps} = total cross-sectional area of prestressing tendons

A_{sp} = cross-sectional area of spiral confinement in beam compression zone

b = beam width

c = section distance from extreme compression fiber to neutral axis

D = diameter of confinement spiral

E_c = concrete modulus of elasticity

E_s = steel modulus of elasticity

F_{cr} = lateral force corresponding to M_{cr}

f_c' = compression strength of unconfined concrete

f_{cc}' = compression strength of confined concrete

f_ℓ = lateral confining stress

f_{si} = initial stress in prestressing tendon (after losses)

$f_{s\ell p}$ = stress in prestressing tendon at limit of proportionality

F_y = frame yield force

f_y = yield strength of spiral confinement

G = concrete shear modulus

h_b = beam depth

h_c = column depth

ℓ_b = beam length (defined in Fig. 3)

ℓ_c = column length (defined in Fig. 3)

$M_1, M_2,$
M_3 = characteristic moments on force-deformation curve (see Fig. 5)

M_{cr} = cracking moment

R_w = force reduction factor (from Ref. 3)

S = soil type (from Ref. 3)

s = pitch of spiral confinement

T = fundamental period of frame

T_i = initial total prestressing force

W = seismic weight of building

x = length of debonding in beam

α, β = parameters describing equivalent compression stress block (defined in Fig. 6)

$\Delta_1, \Delta_2,$
Δ_3 = displacements corresponding to M_1, M_2, M_3

Δ_ℓ = extension of debonded prestressing tendon

Δ_u = ultimate displacement

Δ_y = yield displacement

$\Delta\varepsilon_s$ = change in steel strain

ε_s = steel strain

μ_Δ = displacement ductility factor, defined by Eq. (11)

θ = drift angle

APPENDIX B — ANALYSIS OF A
DEBONDED PRECAST, PRESTRESSED CONCRETE JOINT

A deep-membered precast joint unit, forming part of an external one-way moment-resisting frame, is considered. As shown in Fig. B1, the bay length is 25 ft (7.62 m), story height is 12 ft (3.66 m), beam size is 48 x 24 in. (1220 x 610 mm) and the column cross section is 54 x 30 in. (1370 x 760 mm).

The compression zones of the beam ends are confined with intersecting spirals of #4 (12.7 mm) bars at 3 in. (76 mm) pitch, 14 in. (356 mm) diameter over the end 4 ft (1220 mm) and prestressing ducts are supported by stirrups close to midheight as shown.

The prestress is debonded through the joint, and for a distance of 48 in. (1220 mm) on either side. The beam prestress provides 864 kips (3840 kN) force at 120 ksi (828 MPa) after losses. The prestress limit of proportionality is taken as 200 ksi (1380 MPa). Note that the initial prestress level corresponds to an average prestress of 750 psi (5.18 MPa) in the beam concrete. The concrete unconfined compression strength is 5 ksi (34.5 MPa).

Confined Concrete Strength

The lateral confining stress in the beam compression zone at yield in the spiral reinforcement is given by Eq. (13) as:

$$f_\ell = \frac{2A_{sp}f_y}{Ds}$$
$$= \frac{2 \ x \ 0.2 \ x \ 60}{14 \ x \ 3}$$
$$= 0.57 \ ksi \ (3.93 \ MPa)$$

Thus, from Eq. (12), the confined concrete strength is:

$$f'_c = 5.0 \left[-1.254 \right.$$
$$+ 2.254 \sqrt{1 + \frac{7.94 \ x \ 0.57}{5}}$$
$$\left. - \frac{2 \ x \ 0.57}{5} \right]$$
$$= 8.15 \ ksi \ (54.3 \ MPa)$$

Elastic Deformations

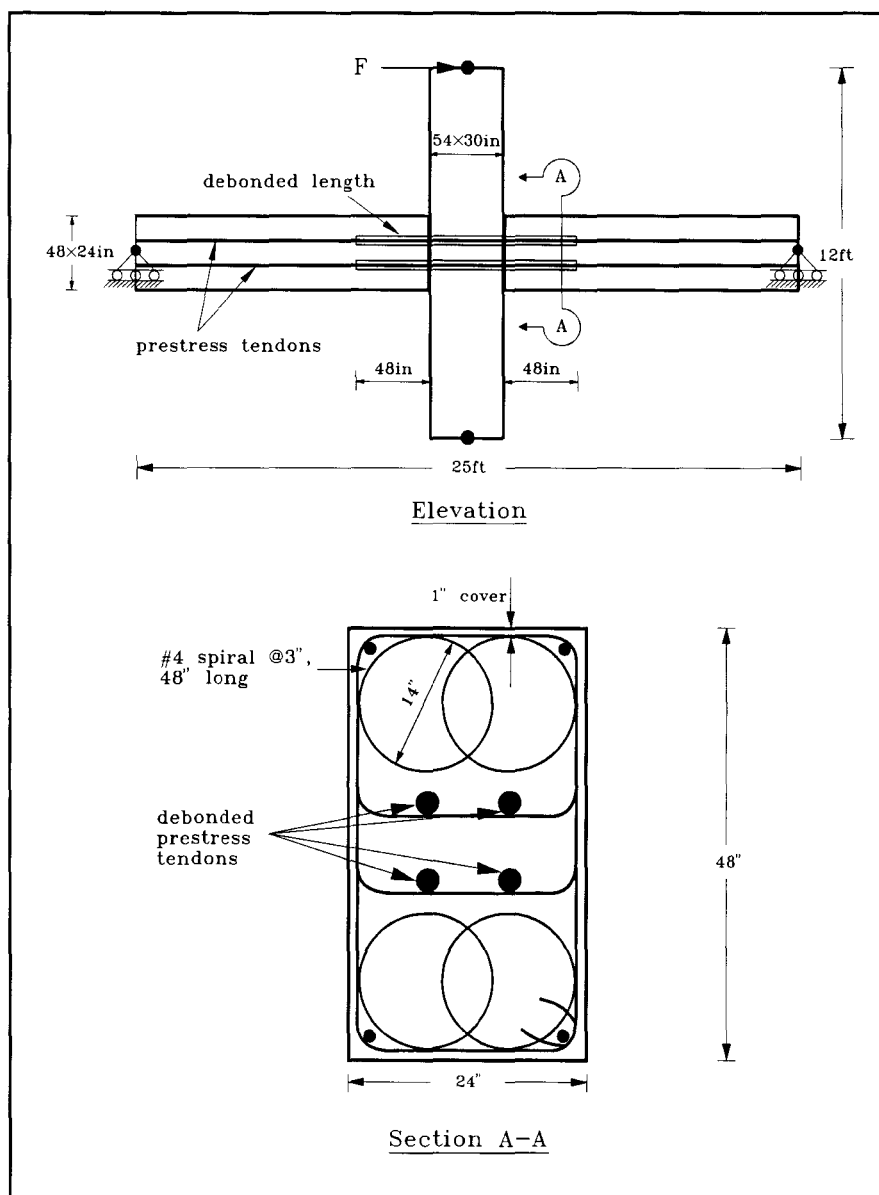At Point 1 on the force-deformation characteristic shown in Fig. 5(b), corresponding to decompression at the extreme tension fiber the moment will be:

$$M = 864 \ x \ \frac{48}{6}$$
$$= 6912 \ kip\text{-}in. \ \ (780 \ kN\text{-}m)$$

The corresponding beam and column shears are 56.2 and 117 kips (250 and 520 kN), respectively. Using these shears, along with an elastic modulus of $E_c = 4 \ x \ 10^6$ psi (27.6 GPa) and shear modulus of $G = 1.74 \ x \ 10^6$ psi (12.0 GPa), the lateral displacement of the column top Δ_1 is found to be 0.099 in. (2.52 mm).

Note that to make some provision for joint shear deformation, no rigid end blocks were assumed in the analysis. Considering the joint size, this may be conservative (i.e., elastic deformations may be a little large).

Taking the lateral force and deformation at Point 2 on the force-deformation curve as twice those at Point 1 (see text of paper), the "yield" force and displacement are:

$$F_y = F_2 = 234 \ kips \ (1041 \ kN)$$
$$\Delta_y = \Delta_2 = 0.198 \ in. \ (5.03 \ mm)$$

Fig B1. Dimensions of example subassemblage.
(Note: 1 ft = 304.8 mm; 1 in. = 25.4 mm.)

The "yield" displacement corresponds to a drift angle of 0.00138 degrees.

Conditions at Maximum Steel Strain

The permitted "ultimate" condition corresponds to a maximum stress of 200 ksi (1380 MPa) in the prestressing strand. The corresponding tension force is:

$$\frac{200}{120} \times 864 = 1440 \text{ kips (6405 kN)}$$

Taking the product $\alpha\beta$ as 0.75 for confined concrete, the depth of the compression zone is given by Eq. (6) as:

$$c = \frac{1440}{0.75 \times 24 \times 8.15}$$

$$= 9.8 \text{ in. (249 mm)}$$

Because of the high compressive strains, spalling of the cover concrete is expected. As a result of the curved shape of the upper surface of the confined core, assume an effective top surface 3 in. (76 mm) below the beam top. The corresponding moment M_3 is, from Eq. (7):

$$M_3 = 1440 (24 - 3 - 4)$$
$$= 24480 \text{ kip-in. [2764 kN-m]}$$

with a corresponding column shear force of $F_3 = 414$ kips (1841 kN)
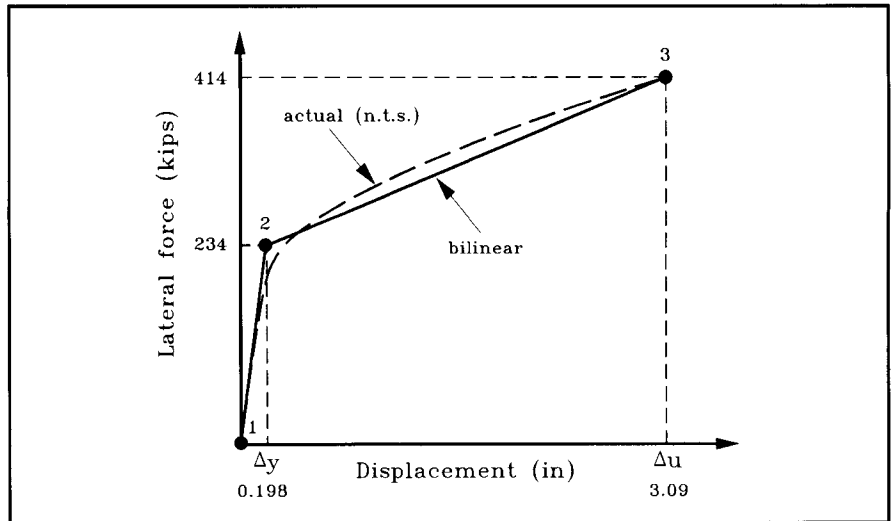

Fig. B2. Force-displacement characteristic for example subassemblage.
(Note: 1 kip = 4.45 kN; 1 in. = 25.4 mm.)

Assuming $E_s = 28 \times 10^6$ psi (193 GPa) for prestressing strand, from Eq. (8):

$$\Delta_\ell = \frac{(200 - 120)}{28,000}(54/2 + 48)$$

$$= 0.214 \text{ in. (5.44 mm)}$$

From Eq. (9), the "plastic" drift angle θ is:

$$\theta = \frac{0.214}{(24 - 3 - 9.8)} = 0.019$$

and the total drift is:

$$\Delta_3 = \Delta_2 \times \frac{414}{234} + 0.019 \times 144$$

$$= 3.09 \text{ in. (78.5 mm)}$$

This displacement corresponds to a drift ratio of 0.0215.

The effective displacement ductility of the assemblage is thus:

$$\mu_\theta = \frac{3.09}{0.198} = 15.6$$

The equivalent bilinear force-deformation relationship is shown in Fig. B2.